

Interaction of fractal processes with linear systems

Original

Interaction of fractal processes with linear systems / GRIVET TALOCIA, Stefano; Canavero, Flavio. - In: PHYSICS LETTERS A. - ISSN 0375-9601. - STAMPA. - 228:4-5(1997), pp. 261-270. [10.1016/S0375-9601(97)00129-1]

Availability:

This version is available at: 11583/1821641 since:

Publisher:

Elsevier

Published

DOI:10.1016/S0375-9601(97)00129-1

Terms of use:

This article is made available under terms and conditions as specified in the corresponding bibliographic description in the repository

Publisher copyright

(Article begins on next page)

Interaction of fractal processes with linear systems

S. Grivet-Talocia*, F. Canavero

*Dipartimento di Elettronica, Politecnico di Torino,
Corso Duca degli Abruzzi 24, 10129, Torino, Italy*

January 7, 1997

Abstract

The interaction of a fractal process with a linear system is investigated. The system is described in terms of its transfer function, which is approximated with an arbitrary number of power-law decay segments. Asymptotic expansions for the scale-dependent fractal dimension are derived. Some examples of common linear systems are illustrated.

PACS: 02.30.Mv, 02.50.Ey, 05.40.+j

Keywords: $1/f^\alpha$ noise. Fractal dimension. Structure functions. Linear systems.

*Corresponding author: S. Grivet-Talocia, Dipartimento di Elettronica, Politecnico di Torino, Corso Duca degli Abruzzi 24, 10129, Torino, Italy. Tel: +39-11-564-4104. Fax: +39-11-564-4015. E-mail: grivet@polito.it

1 Introduction

The family of processes commonly referred to as $1/f^\alpha$ occur in many fields of applications [1]. Examples range from geophysical [2] and economical [3] signals to noise in electronic circuits [4]. An extensive collection of references can be found in [5]. The ability to model these processes with few significant parameters is therefore of great interest. This is not a trivial task, because of the long range correlations in the signals and their intrinsic non-stationarity.

Approaches based on the self-similarity of the curves obtained by plotting the graph of a realization of the process have been investigated [6]. The basic parameter is the fractal dimension D [7], which quantifies the degree of irregularity of the graph [8]. For a curve in the plane, D can range from 1 to 2 [8, 9]. It can be shown that D is related to the spectral slope through $\alpha = 5 - 2D$ [10]. Another common quantity associated with $1/f^\alpha$ processes is the parameter H [11], defined as the scaling exponent for the so-called structure functions (see section 2). The relationship with the fractal dimension $D = 2 - H$ is well known.

It has been shown in [12] that the relationship between fractal dimension and spectral slope holds only in an approximate sense when considering a bandlimited fractal process. High and low frequency cutoffs are necessary to limit the total energy of the process, and are indeed intrinsic in finite length sampled time series. They introduce correcting terms in the fractal exponent, that depend on the particular scale being considered.

This work deals with a generalization of the model proposed in [12]. The fractal characterization of a process at the output of a linear system is sought for. This is a problem commonly encountered in various applications, because most data are made available through a measurement process that involves some kind of filtering. This additional processing is sometimes designed, but often unwanted and spurious. The measured data can often be modeled as the output of a generic linear system. The dependence of the fractal dimension on a quite general kind of linear system will be investigated. The model of the

output process is based on an approximation of the transfer function of the system with an arbitrary number of power law decay segments and is outlined in section 2. The fractal exponent $H(T)$ is estimated in the proper scaling range for the general case by means of asymptotic expansions (section 3). Section 4 illustrates the validity of the derived expressions comparing the behavior of $H(T)$ with numerical estimates, while section 5 is devoted to the discussion of the results.

2 The fractal model

Let us recall that the fractal dimension of a signal x_t is a real number $D = 2 - H$, where H is defined as the scaling exponent of the structure function

$$\sigma_T^2 = \langle (x_t - x_{t-T})^2 \rangle \sim T^{2H}. \quad (1)$$

If the power spectrum $P_x(f)$ of the process is known, the structure function σ_T can be evaluated [13] as

$$\sigma_T^2 = 4 \int_0^\infty P_x(f) \sin^2(\pi f T) df. \quad (2)$$

A typical fractal signal is characterized by a spectrum with a power-law decay in frequency, $P_x(f) \sim f^{-\alpha}$. The total energy of such a process, however, is infinite. This is the main reason why a bandlimited model for a fractal process has been considered in [13]. On the other hand, the presence of low and high frequency cutoffs introduces [12] a series of correcting terms on the scaling exponent H . It becomes then necessary to define a scale-dependent exponent

$$H(T) = \frac{T}{2\sigma_T^2} \frac{d}{dT} \sigma_T^2 \quad (3)$$

to account for these corrections. The scale-dependent fractal dimension can be defined accordingly as $D(T) = 2 - H(T)$.

The reader is referred to [12] for the derivation of asymptotic expansions of $H(T)$ for a simple bandlimited fractal process. The aim of this paper is to provide a generalization

for those results. We will refer to the situation where a fractal signal x_t is fed to a generic linear system, characterized by its frequency-domain transfer function $G(f)$. The output y_t is the process that will be investigated. The power spectrum of the output signal can be immediately related to the power spectrum of the input through

$$P_y(f) = |G(f)|^2 P_x(f). \quad (4)$$

The model for the process y_t under investigation is fairly general. It is assumed that $P_y(f)$ is partitioned with an arbitrary number of frequency intervals with a uniform power law decay. Both the linear system and the input contribute according to Eq. (4) to this frequency behavior. The general form for $|G(f)|^2$ that is used here is an approximation of the transfer function for a linear system whose dynamics is described by a set of ordinary differential equations with constant coefficients. These systems typically describe electric ‘lumped’ circuits and are characterized by rational transfer functions with a finite number of zeros and poles. When the frequencies of two adjacent singularities (either zeros or poles) are sufficiently far apart, the transfer function modulus squared can be approximated by a power law with integer even slope. This approximation is quite accurate even close to the singularities. A generic fractal process x_t has the same kind of behavior, with a single or multiple power law decay. The slope does not need to be an integer but can be any real number. When combining the transfer function with the input power spectrum according to Eq. (4), we obtain a function $P_y(f)$ that can be approximated by a number of power law decay intervals with arbitrary slope, separated by break points. These break points can be due either to zeros and poles of $G(f)$ or to breaks already present in $P_x(f)$ (see e.g. [12]). This consideration can be further generalized assuming that the input of our system is white noise, and the transfer function is characterized by arbitrary slopes, without the constraint of being integer numbers. In summary, the basic model considered

in this paper is

$$\begin{aligned} P_y(f) &= \left(\frac{f}{f_0}\right)^{-\alpha_0}, & f < f_0 \\ &= C_k \left(\frac{f}{f_{k-1}}\right)^{-\alpha_k}, & f_{k-1} \leq f < f_k, \quad 1 < k < k_{max}, \end{aligned} \quad (5)$$

and is plotted in Fig. 1. We indicated with $\{f_k, k = 0, \dots, k_{max} - 1\}$ the frequencies where the slope changes and with α_k the logarithmic slopes. These can be any real number. It is assumed that adjacent slopes are different and that $\alpha_0 < 1$ to insure a total finite energy. The last frequency break point $f_{k_{max}}$ can be set to infinity. In this case, we must set also $\alpha_{k_{max}} > 1$. Otherwise $\alpha_{k_{max}}$ can be any number because the spectrum is assumed identically zero for $f > f_{k_{max}}$. The constants C_k insure that the spectrum is a continuous function of the frequency, and are expressed by

$$C_k = \prod_{i=1}^{k-1} \left(\frac{f_i}{f_{i-1}}\right)^{-\alpha_i}. \quad (6)$$

It should be noted that a linear system introduces also frequency-dependent phase shifts on the output signal. However, when the input is white noise (or any fractal process), the phase can be assumed to be a random variable uniformly distributed in $[0, 2\pi]$, and any slowly varying phase shift due to $\arg\{G(f)\}$ is negligible on the output.

The process y_t can be characterized by the exponent $H(T)$ only when the scale T is such that

$$\frac{1}{f_k} \ll T \ll \frac{1}{f_{k-1}}. \quad (7)$$

This condition automatically insures that the two frequencies f_{k-1} and f_k are well separated. The nominal value of $H(T)$ in this range is (see [12] and references therein)

$$H(T) = \begin{cases} 0, & \alpha_k < 1, \\ \frac{1}{2}(\alpha_k - 1), & \alpha_k \in [1, 3], \\ 1, & \alpha_k > 3. \end{cases} \quad (8)$$

We will show in section 3 that the expressions in Eq. 8 are true only in an approximate sense, because the form of $P_y(f)$ outside the interval $[f_{k-1}, f_k]$ introduces scale-dependent corrections. Asymptotic expansions for these corrections are also explicitly derived. The case that was studied in [12] can be found as a particular case setting $k_{max} = 2$, $k = 1$, $\alpha_0 = 0$, and $\alpha_2 \rightarrow \infty$.

3 Derivation of the scaling exponent

This section is devoted to the analytical derivation of the scaling exponent $H(T)$ from the model of the spectrum $P_y(f)$ in Eq. (5). This will be done evaluating the structure function σ_T^2 defined in Eq. (2) and then using Eq. (3). Without loss of generality we will restrict the analysis to those scales T satisfying Eq. (7). Different scaling regimes can be selected by changing the parameter k . It is necessary that the closest break frequencies are sufficiently separated to be able to model the process as a fractal. If this condition is satisfied the following approximations can be made without further restrictions.

It will be shown that $H(T)$ depends mainly on the slope α_k in the frequency band $[f_{k-1}, f_k]$. The low and high frequency bands are responsible for the scale dependence of the fractal dimension of the process. It is convenient then to split the structure function σ_T^2 into three basic contributions for low, intermediate, and high frequency, and to apply Eq. (2) separately. We have

$$\sigma_T^2 = (\sigma_T^2)_{LF} + (\sigma_T^2)_{MF} + (\sigma_T^2)_{HF}, \quad (9)$$

where

$$(\sigma_T^2)_{LF} = 4 \int_0^{f_{k-1}} P_y(f) \sin^2(\pi f T) df, \quad (10)$$

$$(\sigma_T^2)_{MF} = 4 \int_{f_{k-1}}^{f_k} P_y(f) \sin^2(\pi f T) df, \quad (11)$$

$$(\sigma_T^2)_{HF} = 4 \int_{f_k}^{f_{k_{max}}} P_y(f) \sin^2(\pi f T) df. \quad (12)$$

These three contributions will now be examined in detail.

Let us consider first the low frequency contribution. Substituting the explicit expression for the spectrum we have

$$\begin{aligned}
(\sigma_T^2)_{LF} &= 4 \int_0^{f_0} \left(\frac{f}{f_0} \right)^{-\alpha_0} \sin^2(\pi f T) df \\
&+ 4 \sum_{m=1}^{k-1} C_m \int_{f_{m-1}}^{f_m} \left(\frac{f}{f_{m-1}} \right)^{-\alpha_m} \sin^2(\pi f T) df,
\end{aligned} \tag{13}$$

where $\pi f_m T \ll 1 \quad \forall m$. The integrals can then be approximated by expanding the sine function for small values of its argument. The final result, obtained with a fourth order expansion, is

$$\begin{aligned}
(\sigma_T^2)_{LF} &\simeq \sum_{m=1}^{k-1} f_{m-1} C_m (\alpha_{m-1} - \alpha_m) \left[\frac{(2\pi f_{m-1} T)^2}{(3 - \alpha_{m-1})(3 - \alpha_m)} - \frac{(2\pi f_{m-1} T)^4}{12(5 - \alpha_{m-1})(5 - \alpha_m)} \right] \\
&+ f_{k-1} C_k \left[\frac{(2\pi f_{k-1} T)^2}{(3 - \alpha_{k-1})} - \frac{(2\pi f_{k-1} T)^4}{12(5 - \alpha_{k-1})} \right].
\end{aligned} \tag{14}$$

This expression is valid for $\alpha_m \neq 3, 5 \quad \forall m < k$. It can be shown that if $\alpha_p \rightarrow 3$ with $p < k$ the two singular terms in Eq. (14) containing $(3 - \alpha_p)$ in the denominator cancel out and should be substituted with the expression

$$f_{p-1} C_p (2\pi f_{p-1} T)^2 \left[\frac{\alpha_{p-1} - \alpha_{p+1}}{(3 - \alpha_{p-1})(3 - \alpha_{p+1})} + \log \left(\frac{f_p}{f_{p-1}} \right) \right]. \tag{15}$$

This expression is not singular because the slopes α_{p-1} and α_{p+1} are different from $\alpha_p = 3$ according to the assumptions made in section 2. The same argument can be applied if $\alpha_p = 5$. Without loss of generality we will suppose in the following not to be in these particular cases.

Let us consider now the high frequency contribution, expressed by

$$(\sigma_T^2)_{HF} = 4 \sum_{m=k+1}^{k_{max}} C_m \int_{f_{m-1}}^{f_m} \left(\frac{f}{f_{m-1}} \right)^{-\alpha_m} \sin^2(\pi f T) df, \tag{16}$$

where $\pi f_{m-1}T \gg 1 \forall m$. We can split each integral into two parts using the identity $2\sin^2 \xi = 1 - \cos(2\xi)$. The constant part with respect to T can be evaluated immediately. The other part can be approximated by integrating by parts keeping the cosine as the integral factor. This operation has the effect of lowering the exponent by one for each integration. After two steps we obtain the complete expression

$$\begin{aligned}
(\sigma_T^2)_{HF} \simeq & -2f_k C_{k+1} \left[\frac{1}{1-\alpha_k} - \frac{\sin(2\pi f_k T)}{(2\pi f_k T)} + \alpha_{k+1} \frac{\cos(2\pi f_k T)}{(2\pi f_k T)^2} \right] \\
& + 2 \sum_{m=k+2}^{k_{max}} f_{m-1} C_m (\alpha_{m-1} - \alpha_m) \left[\frac{1}{(1-\alpha_{m-1})(1-\alpha_m)} + \frac{\cos(2\pi f_{m-1} T)}{(2\pi f_{m-1} T)^2} \right] \\
& + 2f_{k_{max}} C_{k_{max}+1} \left[\frac{1}{1-\alpha_{k_{max}}} - \frac{\sin(2\pi f_{k_{max}} T)}{2\pi f_{k_{max}} T} + \alpha_{k_{max}} \frac{\cos(2\pi f_{k_{max}} T)}{(2\pi f_{k_{max}} T)^2} \right],
\end{aligned} \tag{17}$$

valid when $f_{k_{max}} < \infty$ and $\alpha_m \neq 1 \forall m \geq k$. If $f_{k_{max}} = \infty$ we have $C_{k_{max}+1} = 0$, and the last term in the preceding expression disappears. If $\alpha_p = 1$ for some $p > k$ we can proceed as indicated above. Taking the two terms with $(1-\alpha_p)$ at the denominator and combining them, a cancellation of the singularity occurs, and the resulting expression to be substituted into Eq. (17) reads

$$2f_{p-1} C_p \left[\frac{\alpha_{p-1} - \alpha_{p+1}}{(1-\alpha_{p-1})(1-\alpha_{p+1})} + \log \left(\frac{f_p}{f_{p-1}} \right) \right]. \tag{18}$$

The last contribution to be considered is $(\sigma_T^2)_{MF}$. This is the main term, which is responsible for the asymptotic fractal scaling of the process. We will investigate first the case $\alpha_k \in (1, 3)$, that corresponds to a non-integer value of the fractal dimension. In this range the integral converges when the integration interval is set to $(0, \infty)$ and can be evaluated in a closed form, while the contributions due to the finiteness of the integration interval can be approximated separately and subtracted. Using the results in [12] we obtain

$$(\sigma_T^2)_{MF} \simeq -2f_{k-1} C_k \Gamma(1-\alpha_k) \sin \left(\frac{\alpha_k \pi}{2} \right) (2\pi f_{k-1} T)^{\alpha_k-1}$$

$$\begin{aligned}
& - f_{k-1} C_k \left[\frac{(2\pi f_{k-1} T)^2}{3 - \alpha_k} - \frac{(2\pi f_{k-1} T)^4}{12(5 - \alpha_k)} \right] \\
& + 2f_k C_{k+1} \left[\frac{1}{1 - \alpha_k} - \frac{\sin(2\pi f_k T)}{(2\pi f_k T)} + \alpha_k \frac{\cos(2\pi f_k T)}{(2\pi f_k T)^2} \right].
\end{aligned} \tag{19}$$

Finally, combining Eqs. (14), (17) and (19), we obtain the complete expression for the approximate structure function

$$\begin{aligned}
\sigma_T^2 & \simeq \sum_{m=1}^k f_{m-1} C_m (\alpha_{m-1} - \alpha_m) \left[\frac{(2\pi f_{m-1} T)^2}{(3 - \alpha_{m-1})(3 - \alpha_m)} - \frac{(2\pi f_{m-1} T)^4}{12(5 - \alpha_{m-1})(5 - \alpha_m)} \right] \\
& - 2f_{k-1} C_k \Gamma(1 - \alpha_k) \sin\left(\frac{\alpha_k \pi}{2}\right) (2\pi f_{k-1} T)^{\alpha_k - 1} \\
& + 2 \sum_{m=k+1}^{k_{max}} f_{m-1} C_m (\alpha_{m-1} - \alpha_m) \left[\frac{1}{(1 - \alpha_{m-1})(1 - \alpha_m)} + \frac{\cos(2\pi f_{m-1} T)}{(2\pi f_{m-1} T)^2} \right] \\
& + 2f_{k_{max}} C_{k_{max}+1} \left[\frac{1}{1 - \alpha_{k_{max}}} - \frac{\sin(2\pi f_{k_{max}} T)}{2\pi f_{k_{max}} T} + \alpha_{k_{max}} \frac{\cos(2\pi f_{k_{max}} T)}{(2\pi f_{k_{max}} T)^2} \right].
\end{aligned} \tag{20}$$

The modifications that are necessary when $\alpha_m = 1, 3$ and 5 for $m \neq k$ have already been discussed. The cases $\alpha_k = 1, 3$ will be analyzed in the following paragraphs. Also, the singularity of the Γ function for $\alpha_k = 2$ is only apparent due to a cancellation with the zero of the sine function in the same factor (see [12]).

Combining now Eqs. (20) and (3) we can evaluate the scaling exponent $H(T)$ for $1 < \alpha_k < 3$. The result is

$$H(T) \simeq \frac{\alpha_k - 1}{2} + \frac{N(T)}{\sigma_T^2}, \tag{21}$$

where

$$\begin{aligned}
N(T) & = \sum_{m=1}^k f_{m-1} C_m (\alpha_{m-1} - \alpha_m) \left[\frac{(3 - \alpha_k)(2\pi f_{m-1} T)^2}{2(3 - \alpha_{m-1})(3 - \alpha_m)} - \frac{(5 - \alpha_k)(2\pi f_{m-1} T)^4}{24(5 - \alpha_{m-1})(5 - \alpha_m)} \right] \\
& + \sum_{m=k+1}^{k_{max}} f_{m-1} C_m (\alpha_{m-1} - \alpha_m) \left[\frac{1 - \alpha_k}{(1 - \alpha_{m-1})(1 - \alpha_m)} - \frac{\sin(2\pi f_{m-1} T)}{(2\pi f_{m-1} T)} \right] \\
& + f_{k_{max}} C_{k_{max}+1} \left[\frac{\alpha_k - 1}{\alpha_{k_{max}} - 1} - \cos(2\pi f_{k_{max}} T) + (\alpha_k - \alpha_{k_{max}}) \frac{\sin(2\pi f_{k_{max}} T)}{2\pi f_{k_{max}} T} \right].
\end{aligned} \tag{22}$$

This expression is valid for $\alpha_m \neq 1, 3, 5 \forall m \neq k$. These particular cases can be treated in

the same way as above.

The asymptotic behavior of $H(T)$ can be found by reducing the influence of the low and high frequency break points. It is sufficient to set

$$2\pi f_{k-1}T \rightarrow 0, \quad (23)$$

$$\frac{f_{k-1}}{f_k} \rightarrow 0, \quad (24)$$

because $f_{m-1} < f_m \forall m$. If $\alpha_k \in (1, 3)$ the scale dependent correction in Eq. (21) vanishes, and the fractal exponent assumes the nominal value $H(T) \simeq \frac{1}{2}(\alpha_k - 1)$.

Let us consider now the cases $\alpha_k = 1$ and $\alpha_k = 3$. It can be easily shown with series expansions that the singularities in σ_T^2 cancel out. The structure functions are, respectively, expressed by

$$\begin{aligned} \sigma_T^2|_{\alpha_k \rightarrow 3} &\simeq \sum_{m=1}^{k-1} f_{m-1} C_m (\alpha_{m-1} - \alpha_m) \left[\frac{(2\pi f_{m-1}T)^2}{(3 - \alpha_{m-1})(3 - \alpha_m)} - \frac{(2\pi f_{m-1}T)^4}{12(5 - \alpha_{m-1})(5 - \alpha_m)} \right] \\ &+ f_{k-1} C_k \left[\frac{1}{3 - \alpha_{k-1}} + \Psi(3) - \log(2\pi f_{k-1}T) \right] (2\pi f_{k-1}T)^2 \\ &- f_{k-1} C_k \frac{\alpha_{k-1} - \alpha_k}{12(5 - \alpha_{k-1})(5 - \alpha_k)} (2\pi f_{k-1}T)^4 \\ &+ 2 \sum_{m=k+1}^{k_{max}} f_{m-1} C_m (\alpha_{m-1} - \alpha_m) \left[\frac{1}{(1 - \alpha_{m-1})(1 - \alpha_m)} + \frac{\cos(2\pi f_{m-1}T)}{(2\pi f_{m-1}T)^2} \right] \\ &+ 2 f_{k_{max}} C_{k_{max}+1} \left[\frac{1}{1 - \alpha_{k_{max}}} - \frac{\sin(2\pi f_{k_{max}}T)}{2\pi f_{k_{max}}T} + \alpha_{k_{max}} \frac{\cos(2\pi f_{k_{max}}T)}{(2\pi f_{k_{max}}T)^2} \right] \end{aligned} \quad (25)$$

and

$$\begin{aligned} \sigma_T^2|_{\alpha_k \rightarrow 1} &\simeq \sum_{m=1}^k f_{m-1} C_m (\alpha_{m-1} - \alpha_m) \left[\frac{(2\pi f_{m-1}T)^2}{(3 - \alpha_{m-1})(3 - \alpha_m)} - \frac{(2\pi f_{m-1}T)^4}{12(5 - \alpha_{m-1})(5 - \alpha_m)} \right] \\ &- 2f_k C_{k+1} \left[\frac{1}{1 - \alpha_{k+1}} + \Psi(1) - \log(2\pi f_k T) - (1 - \alpha_{k+1}) \frac{\cos(2\pi f_k T)}{(2\pi f_k T)^2} \right] \\ &+ 2 \sum_{m=k+2}^{k_{max}} f_{m-1} C_m (\alpha_{m-1} - \alpha_m) \left[\frac{1}{(1 - \alpha_{m-1})(1 - \alpha_m)} + \frac{\cos(2\pi f_{m-1}T)}{(2\pi f_{m-1}T)^2} \right] \\ &+ 2 f_{k_{max}} C_{k_{max}+1} \left[\frac{1}{1 - \alpha_{k_{max}}} - \frac{\sin(2\pi f_{k_{max}}T)}{2\pi f_{k_{max}}T} + \alpha_{k_{max}} \frac{\cos(2\pi f_{k_{max}}T)}{(2\pi f_{k_{max}}T)^2} \right], \end{aligned} \quad (26)$$

where $\Psi(z) = d \ln \Gamma(z)/dz$ [14]. The function $N(T)$ is easily evaluated from the previous expressions using the above procedure. When the conditions (23) and (24) are imposed, the fractal exponents tend to their nominal values $H(T)|_{\alpha_k=1} \rightarrow 0$ and $H(T)|_{\alpha_k=3} \rightarrow 1$.

The last two cases to be considered are $\alpha_k < 1$ and $\alpha_k > 3$. According to Eq. (8) the scaling exponent saturates to 0 for $\alpha_k < 1$ and to 1 for $\alpha_k > 3$. The application of the procedure described above allows the derivation of the scale dependent corrections and the proof of the validity for the asymptotic values. The details will not be shown here for the sake of conciseness. Moreover, the application of the fractal geometry to processes with a sharp frequency decay (a smooth curve) or an almost flat spectrum (a quasi-stationary process) is not justified. The fractal dimension would lose its utility in the quantification of the variations of the curve and its scaling behavior. We will proceed to the next section, where the expressions derived for $\alpha_k \in (1, 3)$ are applied to the analysis of some simple linear filters.

4 Examples

This section presents some numerical examples that illustrate how the asymptotic expansions for $H(T)$ can be used to model the process at the output of a linear system. The input signal x_t will be the simple bandlimited fractal process already considered in [12]. Its power spectrum is characterized by a single power law decay $f^{-\alpha}$, limited by two low and high frequency cutoffs. The low frequency cutoff is due to the finite length of the series, and the high frequency one is due to sampling. In particular, we will consider a process with $N = 32768$ samples and sampling time $T_c = 1/N$ s. Therefore, the frequency cutoffs are $f_0 = 1$ Hz and $f_{\max} = N/2$ Hz. These parameters will not change throughout this section.

Four different linear systems will be considered: a first order lowpass filter, a first order highpass filter, a second order bandpass filter, and a fourth order bandpass filter with two resonance peaks. The exponent $H(T)$ will be evaluated both with the expansions derived

in section 3 and numerically, using its definition (see section 2). The numerical estimates are obtained by generating a number $N_r = 20$ of independent realizations of the process y_t with the prescribed power spectrum, calculating $H(T)$ for each realization and averaging the results over the different realizations. The behavior of $P_y(f)$ for $f < f_0$ will be always assumed flat, setting $\alpha_0 = 0$.

Let us consider first a simple lowpass filter with a single pole, located in $f_p = 4096$ Hz. Its transfer function modulus squared is approximately flat for $f < f_p$ and decays as f^{-2} for $f > f_p$. The set of frequency breaks and slopes of the output process y_t are then expressed by

$$\{f_i\}_{i=0}^{K_{\max}} = \{f_0, f_p, f_{\max}\}, \quad (27)$$

$$\{\alpha_i\}_{i=0}^{K_{\max}} = \{0, \alpha, \alpha + 2\}, \quad (28)$$

where $K_{\max} = 2$ and the scaling range $k = 1$ is such that $1/f_p \ll T \ll 1/f_0$. The exponent $H(T)$ is plotted in Fig. 2 for different values of α ranging from 1 to 3. Figure 2

Let us take now a highpass filter with a single pole in $f_p = 16$ Hz. The transfer function modulus squared is now flat for $f > f_p$ and grows as f^2 for $f < f_p$. The set of frequency breaks and slopes of y_t are

$$\{f_i\}_{i=0}^{K_{\max}} = \{f_0, f_p, f_{\max}\}, \quad (29)$$

$$\{\alpha_i\}_{i=0}^{K_{\max}} = \{0, \alpha - 2, \alpha\}, \quad (30)$$

where $K_{\max} = 2$ and the scaling range $k = 2$ is such that $1/f_{\max} \ll T \ll 1/f_p$. The exponent $H(T)$ is reported in Fig. 3. Figure 3

The third system is a bandpass filter with two single poles in $f_L = 8$ Hz and $f_H = 4096$ Hz. The transfer function modulus squared is flat for $f_L < f < f_H$, growing as f^2 for $f < f_L$ and decaying as f^{-2} for $f > f_H$. The set of frequency breaks and slopes of y_t

are in this case

$$\{f_i\}_{i=0}^{K_{\max}} = \{f_0, f_L, f_H, f_{\max}\}, \quad (31)$$

$$\{\alpha_i\}_{i=0}^{K_{\max}} = \{0, \alpha - 2, \alpha, \alpha + 2\}, \quad (32)$$

where $K_{\max} = 3$ and the scaling range $k = 2$ is such that $1/f_H \ll T \ll 1/f_L$. Figure 4 shows the behavior of $H(T)$. An excellent agreement can be noted between the asymptotic expansions and the numerical estimates of $H(T)$ for all the processes described above. Figure 4

The last system that will be considered shows the effect of resonance peaks in the transfer function $|G(f)|^2$. This situation is typically due to pairs of complex poles with a dumping factor close to 0. Even if the frequency behavior is more complex than in the previous systems, it can be approximated with a piecewise linear curve (in logarithmic axes). The approximation error decreases with the number of segments. Consequently, the asymptotic expansions derived in section 3 can also be employed to model the corrections to the fractal scaling due to resonance peaks in the transfer function. As an example, the fractal process x_t described above is passed through a bandpass filter with transfer function plotted in Fig. 5. The cutoff frequencies are $f_L = 8$ Hz and $f_H = 4096$ Hz, while Figure 5 the resonance peaks are 6 dB above the passing band gain. The exponent $H(T)$ has been evaluated like in the previous cases and is plotted in Fig. 6. It should be noted that the Figure 6 peaks induce oscillations in the exponent $H(T)$ at the resonance frequencies. The small discrepancies for large T and α are due to the limited order of approximations of $(\sigma_T^2)_{LF}$. These approximations could be improved with the same procedure followed in section 3 using higher order expansions.

5 Conclusions

We have presented an analytical approach for the analysis of the interaction between fractal processes and linear systems. The fractal modeling is based upon an approximation of the power spectrum of the process at the system output. The basic assumption is that

the spectrum is made of an arbitrary number of power law decay segments, with at least one well defined scaling range. This means that two of the break frequencies where a discontinuity of the logarithmic slope is located are well separated. The scale dependent fractal exponent $H(T)$ has been investigated within this scaling range using asymptotic expansions, which have been validated with numerical estimates.

The main result of this paper is that the nominal fractal scaling holds only in an approximate sense, because of the non-uniformity of the logarithmic slope of the power spectrum. The expansions derived in section 3 include a series of correcting terms that account for this effect and are scale-dependent. These corrections become less important as the scaling range widens.

A quantitative analysis of the plots reported in this work, however, suggests that these corrections are quite significant even when evaluated at scales T far from the limits of the scaling range. Therefore, the use of a fractal exponent to characterize processes measured at the output of a linear system, or in general having a power spectrum with more than a single power law decay, can be misleading. The strong dependence on the scale T shows that the points $(\ln T, \ln \sigma_T)$ do not lie on a straight line, and the definition itself of a scaling exponent could be questionable.

References

- [1] M. S. Keshner, Proc. IEEE 70 (1982) 212
- [2] A. Davis, A. Marshak, W. Wiscombe and R. Cahalan, J. Geophys. Res. 99 (1984) 8055
- [3] C. J. G. Evertsz and K. Berkner, Chaos, Solitons and Fractals 6 (1995) 121.
- [4] J. Rutman, Proc. IEEE 66 (1978) 1048.
- [5] M. S. Taqqu, “A bibliographic guide to self-similar processes and long-range dependence”, in *Dependence in Probability and Statistics* E. Eberlein and M. S. Taqqu Eds. (Birkhauser, Boston, 1986).
- [6] B.B. Mandelbrot and J.W. Van Ness, SIAM Rev. 10 (1968) 422.
- [7] K. Falconer, Fractal Geometry (Wiley, New York, 1990).
- [8] B.B. Mandelbrot, The Fractal Geometry of Nature (Freeman, New York, 1982).
- [9] M. Barnsley, Fractals Everywhere (Academic Press, New York, 1988).
- [10] H.O. Peitgen and D. Saupe, The science of fractal images (Springer, Berlin, 1988)
- [11] J. Feder, Fractals (Plenum, New York, 1988)
- [12] S. Grivet-Talocia, Phys. Lett. A 200 (1995) 264.
- [13] J. Theiler, Phys. Lett. A 155 (1991) 480.
- [14] M. Abramowitz and I. Stegun, Handbook of Mathematical Functions (Dover, New York, 1970).

Figure Captions

Figure 1: Power spectrum $P_y(f)$ of the process under investigation. The slope in each frequency band $[f_{k-1}, f_k]$ is indicated with α_k . Both axes are logarithmically spaced.

Figure 2: Behavior of $H(T)$ for a single pole lowpass filter. The asymptotic expansions (continuous line) and the numerical estimates (circles) are reported for five different values of α . The dotted lines are one standard deviation apart from the mean.

Figure 3: Behavior of $H(T)$ for a single pole highpass filter. The asymptotic expansions (continuous line) and the numerical estimates (circles) are reported for five different values of α . The dotted lines are one standard deviation apart from the mean.

Figure 4: Behavior of $H(T)$ for a bandpass filter with two single poles. The asymptotic expansions (continuous line) and the numerical estimates (circles) are reported for five different values of α . The dotted lines are one standard deviation apart from the mean.

Figure 5: Transfer function modulus squared of a bandpass filter with two resonance peaks.

Figure 6: Behavior of $H(T)$ for the output of the system in Fig. 5. The asymptotic expansions (continuous line) and the numerical estimates (circles) are reported for five different values of α . The dotted lines are one standard deviation apart from the mean.

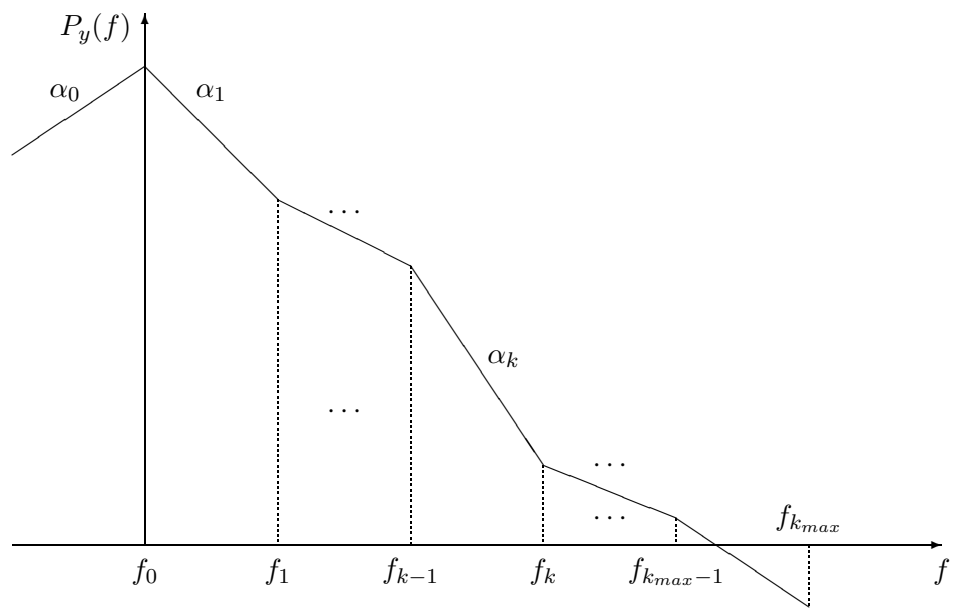


Figure 1:

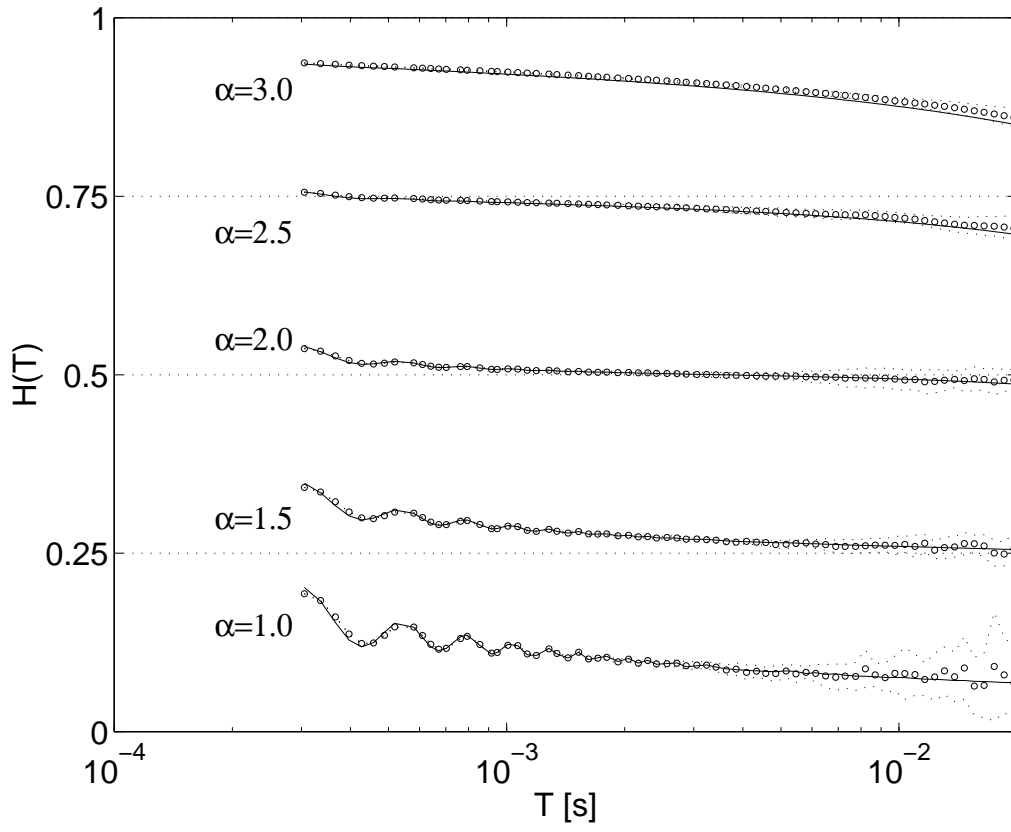


Figure 2:

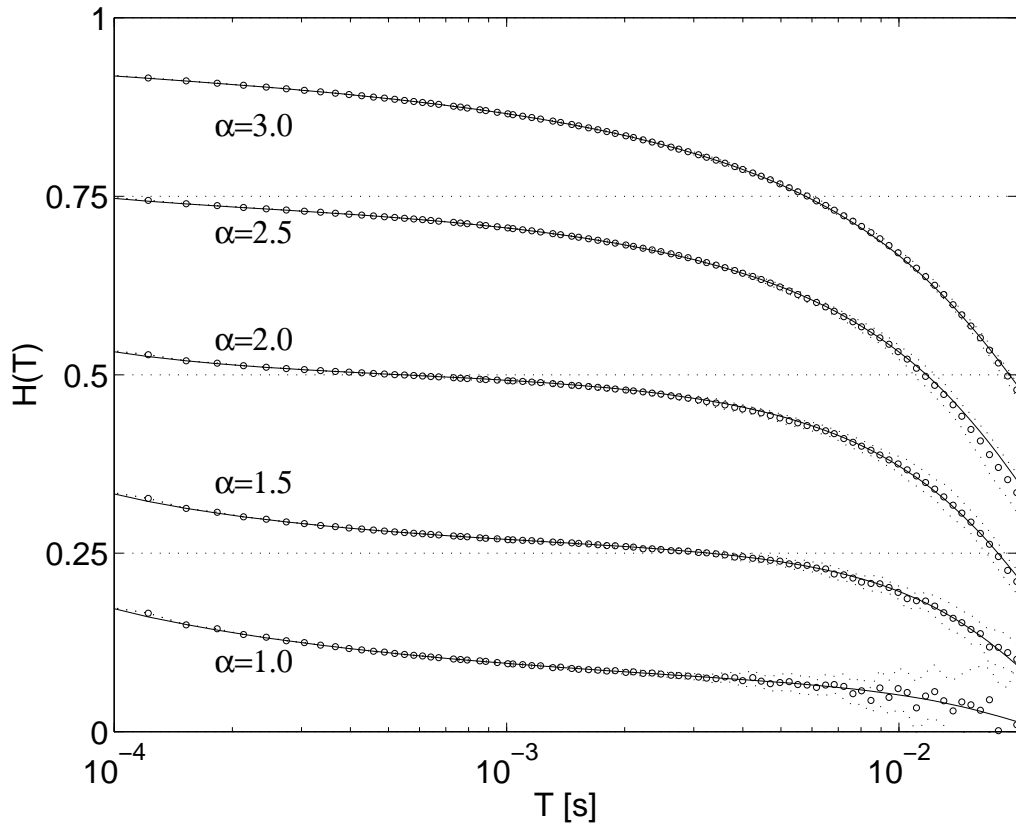


Figure 3:

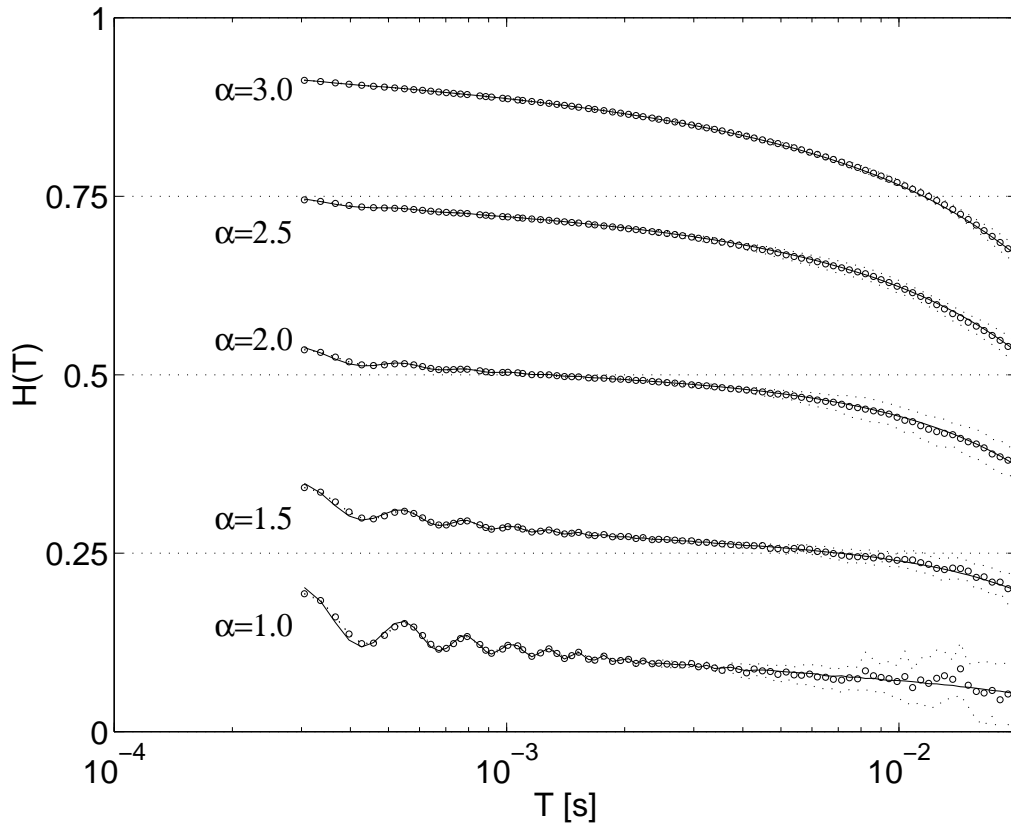


Figure 4:

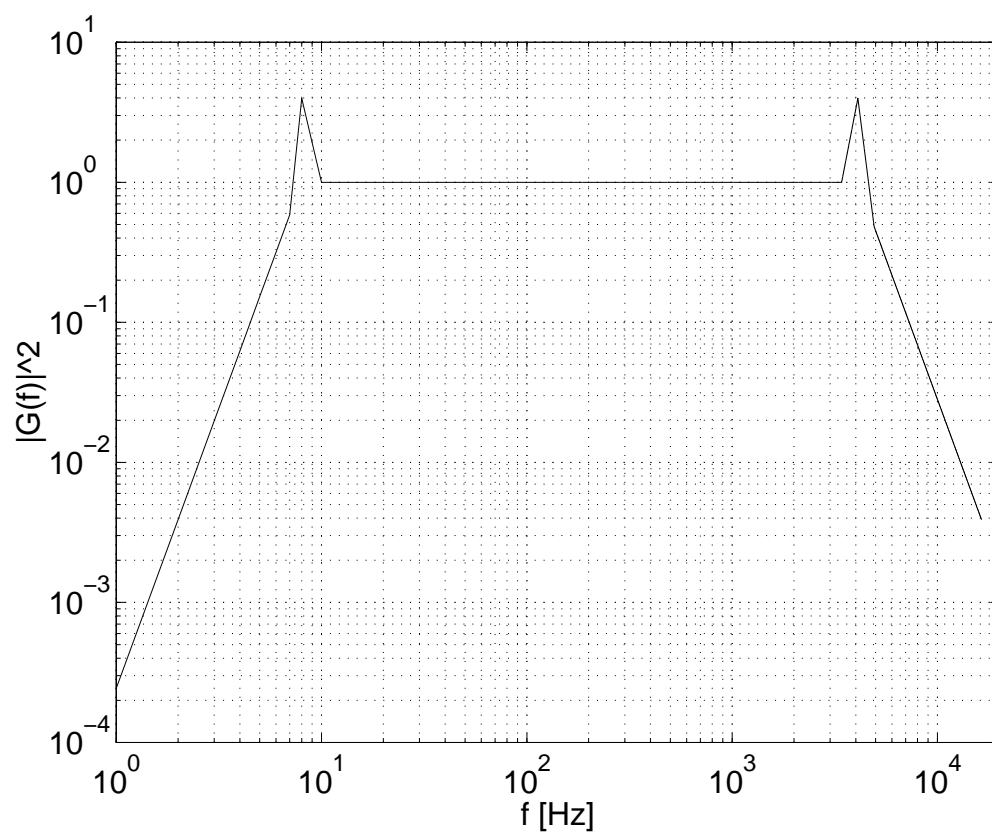


Figure 5:

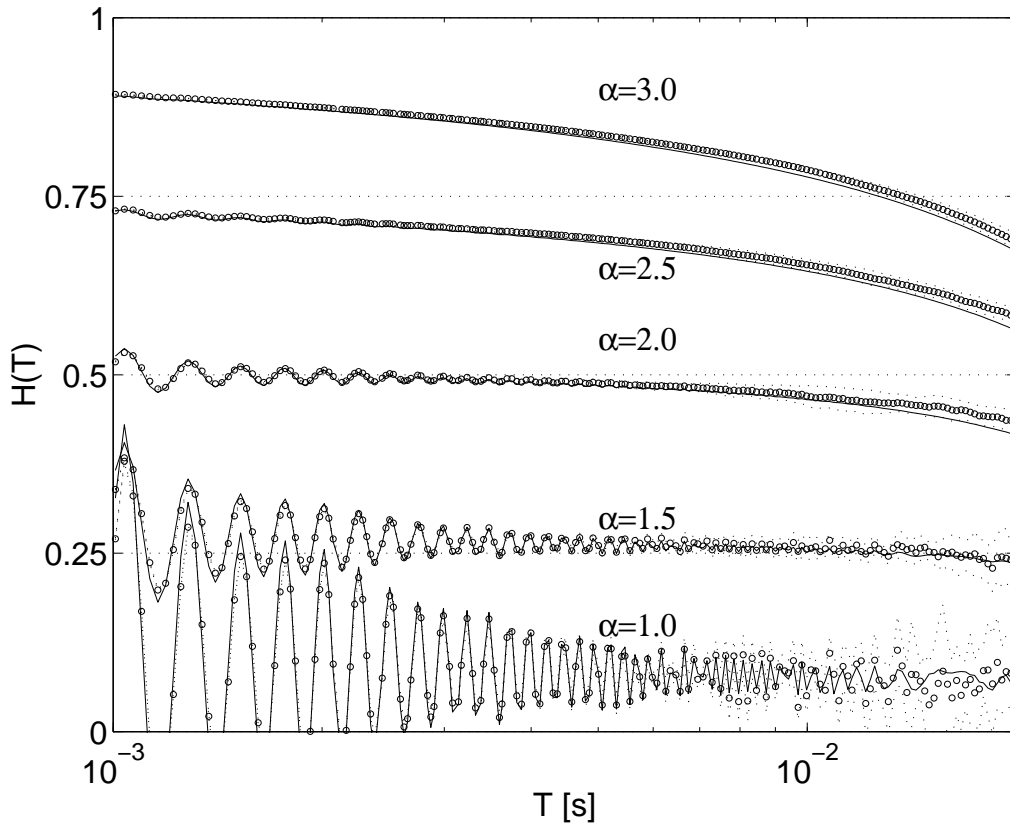


Figure 6: